

# Healing of microcracks in quartz: Implications for fluid flow

Susan L. Brantley

Department of Geosciences, Pennsylvania State University, University Park, Pennsylvania 16802

Brian Evans, Stephen H. Hickman

Department of Earth, Atmospheric, and Planetary Sciences, Massachusetts Institute of Technology, Cambridge  
Massachusetts 02139

David A. Crerar

Department of Geological and Geophysical Sciences, Princeton University, Princeton, New Jersey 08544

## ABSTRACT

Microcracks in quartz  $\sim 100 \mu\text{m}$  in length and  $< \sim 10 \mu\text{m}$  in width heal in 4 h at  $600^\circ\text{C}$  and water pressure of 200 MPa (fluid pressure  $[P_f]$  = confining pressure  $[P_c]$ ). Healing is thermally activated; the activation energy is estimated to be between 80 and 35 kJ/mol, depending on the model assumed. Rates also show dependence on fluid pressure, chemistry, and crack dimensions. Faster healing rates are observed in smaller cracks. Thus, when new cracks are not being produced in rocks at elevated temperatures and pressures, fractures will have a vast range of lifetimes: macrofractures transport most of the fluid volume and seal relatively slowly, whereas microcracks allow pervasive penetration of fluid into the rock mass but heal quickly.

## INTRODUCTION

Several petrologic and chemical analyses of metamorphic rocks suggest that large fluid volumes are necessary to explain the observed modal abundances of minerals (e.g., Ferry, 1986). Walther and Orville (1982) and Walther and Wood (1984) have discussed fluid flow through channels and grain boundaries, diffusion through fluid films on grain boundaries, diffusion along grain boundaries, and the implications of these transport pathways on metamorphic reaction kinetics. Many physical properties of rocks, including the elastic moduli, seismic attenuation, permeability, and electrical resistivity, depend on the volume and morphology of porosity (e.g., Simmons and Richter, 1976; Heard and Page, 1982; Walder and Nur, 1984). Clearly, understanding the permeability of rock and how it changes with time is important.

Connected pore networks may be produced by temperature changes, fluid-pressure cycling, volume changes during metamorphism, nonhydrostatic stresses, and fluid infiltration (e.g., Heard and Page, 1982; Walther and Orville, 1982; Martin, 1972; Watson and Brenan, 1987). Examples of network-reducing mechanisms include crack healing, crack sealing, plastic flow, and pressure solution (see Walder and Nur, 1984). Undersaturated or oversaturated fluids may circulate through a formation and cause net dissolution or precipitation of minerals along fluid pathways. Dissolved material may also be transported locally through a stagnant fluid by solution transfer driven by gradients in chemical potential arising from heterogeneities in distributions of strain, stress, surface energy, or composition.

Where the porosity is of nonequilibrium shape (e.g., cracklike), gradients in chemical potential due to surface tension will always exist and may result in crack healing. Healed fractures in rocks are ubiquitous (e.g., Simmons and Richter, 1976; Roedder, 1981). However, healing rates for minerals at crustal temperatures are not well known. Here we report microcrack-healing rates in quartz in a stagnant fluid at  $400\text{--}600^\circ\text{C}$  with fluid pressure equal to lithostatic pressure ( $\approx 200$  MPa). In more complicated situations, e.g., rocks involved in nonhydrostatic stresses, flowing fluids, or metamorphic reactions, the rate of production of porosity will be the net sum of that due to all the porosity-producing mechanisms minus that due to porosity-reducing mechanisms.

## CRACK-HEALING KINETICS

Surface-curvature-driven healing proceeds in several stages (e.g., Roedder, 1984; Smith and Evans, 1984). Healing of an initially open

crack results in regression of the crack tip either as a continuous front or with the formation of tubular voids and isolated bubbles. Cylindrical tubes, if formed, are unstable to critical perturbations in their radius and neck down (ovulate) into trains of spherical inclusions (Smith and Evans, 1984).

Evans and Charles (1977) formulated a model for healing kinetics assuming isotropic surface tension, parabolic crack shape, ovulation via surface diffusion as the rate-limiting step, local conservation of pore volume, and an untested relation between cylinder spacing and crack aperture. In a slightly modified model treating cracks of elliptical cross section, Hickman and Evans (1987) predicted the regression distance,  $a-r$ , to be proportional to a fractional power of the elapsed time,  $t$ , early in healing:

$$\frac{a-r}{a} \cong E_m \left( \frac{t \exp\left(-\frac{Q}{RT}\right)}{Tab_r^w} \right)^n, \quad (1)$$

where  $r$  is the distance from the center of the crack to the healing front,  $E_m$  includes several constants and material properties,  $Q$  is the activation energy for surface diffusion,  $R$  is the gas constant,  $T$  is the temperature,  $a$  and  $b_r$  are the semi-major and semi-minor axes of the original ellipse, and  $w$  and  $n$  are constants depending on the geometry of cylinder formation. Unfortunately, both models assume a surface-diffusion mechanism; the kinetics for solution-precipitation control are unknown. Until rigorous treatment of fluid-assisted crack healing is available, equation 1 can be used as a model to constrain healing rates.

## HEALING EXPERIMENTS IN QUARTZ

We conducted experiments on rectangular prisms of inclusion-free single crystals of Arkansas quartz in an internally heated gas vessel (Table 1). Prisms ( $\sim 2 \text{ mm} \times 2 \text{ mm} \times 10 \text{ mm}$ ) were cleaned, rinsed, thermally shocked by heating to about  $300^\circ\text{C}$ , and quenched in distilled deionized water (DDW). Crystals and DDW were packed inside a small chamber between mullite frits within an annular alumina capsule, heated to 400, 500, or  $600^\circ\text{C}$ , and adjusted to run pressure. In the shortest duration experiments, thermal transients may have been present, resulting in temperature gradients across the sample chamber from  $\pm 4^\circ\text{C}$  ( $t > 2$  h) to  $\pm 25^\circ\text{C}$  ( $t < 2$  h).

Regression distances, defined as the distance from the smallest observable bubble ( $\sim 1 \mu\text{m}$ ) to the edge of the open crack, were measured in several cracks in each sample by using a transmitted light microscope (Table 1). Also summarized are sequential measurements made on the right (R) and left (L) half of two cracks (KLS1 and KLS2) in quartz (Shelton and Orville, 1980; K. Shelton, 1985, personal commun.). Although the effects of crack size or shape upon healing rates were not explicitly addressed in this study, a rapid decrease in healing rates with increasing crack aperture has been observed both in the calcite/ $\text{CO}_2$  system (Hickman and Evans, 1987) and in the halite/brine system (Hickman and Evans, unpub. manuscript). Extensive healing occurred in what appeared to be the thinnest cracks, whereas cracks with greater apparent apertures were more resistant to healing, in qualitative agreement both with the results of Hickman and Evans and with equation 1. On the basis

of observed fluid-inclusion diameters, crack width appeared to vary between approximately 1 and 10  $\mu\text{m}$ .

## DISCUSSION

Healing in fluid-filled cracks in quartz is rapid above 400 °C and is thermally activated (Fig. 1; Smith and Evans, 1984). Significant healing occurred at 600 °C at 200 MPa water pressure in times as short as 0.25 h. Decreasing fluid pressure appeared to reduce healing rates; no measurable healing was observed for the two 0.5 h experiments at 500 °C and 150 MPa.

### Experimental Repeatability

The large standard deviations in  $a - r$  probably reflect uncontrolled variations in crack shape, crack aperture, fluid chemistry, and possibly

residual stresses. Size and shape are particularly important, and healing rates vary considerably with position in a given crack. In our sample chamber, quartz dissolution is probably retarded by Cu, Fe, and Al impurities (see Iler, 1979). Smith and Evans (1984) used gold capsules, but their pore fluids contained a concentrated Si solution (780 ppm  $\text{SiO}_2$  in 400 °C and 0–2290 ppm  $\text{SiO}_2$  in 600 °C experiments). Increased silica concentration may result in shorter healing time (Bodnar and Sterner, 1987).

In these and earlier experiments, the cracks were not loaded externally during healing (i.e.,  $P_c = P_f$ ). However, some residual internal stresses may remain after fracture formation because the cracks are introduced by thermal shock. Thus, mechanical forces introduced during heating and quenching could also affect rates. Furthermore, in the cold-seal experiments of Smith and Evans (1984), new cracks were probably introduced during each experiment.

### Temperature Effects

We have used our data from Table 1 to estimate the value of the exponent  $n$  in equation 1. A linear regression of all the raw data (rather than the averages presented in Table 1) yields  $n = 0.28 \pm 0.12$  at 400 °C,  $0.46 \pm 0.15$  at 500 °C, and  $0.39 \pm 0.09$  at 600 °C. Within these error estimates (90% confidence) the values are equal:  $n = 0.4 \pm 0.1$ . Regression of Shelton and Orville's data gives  $n = 0.454 \pm 0.005$ ; the lower error probably reflects the fact that crack-width variations were reduced.

At least two models for temperature dependence exist:

$$(a - r) \propto \left\{ \left( \frac{1}{T} \right) \exp \left( -\frac{Q}{RT} \right) \right\}^n, \quad (2)$$

and

$$(a - r) \propto \exp \left( -\frac{Q^*}{RT} \right). \quad (3)$$

Equation 2, derived from equation 1, is suggested by theory and experiments for the surface-diffusion case. Equation 3 assumes a power-law dependence on time and a normal Arrhenius dependence on temperature ( $\{(a - r) \propto t^n \exp(-Q^*/RT)\}$  where  $Q^*$  is an apparent activation energy). By using  $n = 0.4$  for all results,  $Q$  can be determined by linear regression of  $\ln \{(a - r)^{1/n} T t^{-1}\}$  versus  $1/T$  (Fig. 2A):  $Q = 80$  kJ/mol. Similarly,  $Q^*$  can be obtained by evaluating  $\ln(a - r)$  at constant elapsed time as a function of  $1/T$  (Fig. 2B):  $Q^* = 35$  kJ/mol. Both these values are higher than the activation energy for diffusion through an aqueous solution (~21 kJ/mol; Lasaga, 1984).

The distilled water experiments of Smith and Evans (1984), using  $n = 0.4$ , are included in Figure 2A. An upper bound for  $\ln \{(a - r)^{1/n} T t^{-1}\}$  at 200 °C from Smith and Evans' sample QS-31 (starting solution 85 ppm  $\text{SiO}_2$ ) is also plotted, assuming  $a - r < 5 \mu\text{m}$ . We also show two calculated values estimated from the fluid-inclusion syntheses of Bodnar and Sterner. These workers reported microcrack healing of thermally cracked quartz in water at 300 °C in about 10 days (Bodnar and Sterner, 1985) and at 200 °C in about 90 days (Sterner and Bodnar, 1984). Assuming  $n = 0.4$

TABLE 1. HEALED CRACK REGRESSION DISTANCES

Sample*	Run time (h)	Regression distance ( $\mu\text{m}$ )	Number of Observations
$T = 600 \text{ }^\circ\text{C}$ , $P_f = 200 \text{ MPa}$			
3785	6	$184 \pm 64$	9
3685	4	$97 \pm 62$	4
3585	2	$50 \pm 10$	3
31685	0.5	$39 \pm 25$	7
31885	0.25	$76 \pm 58$	6
7885	0.25	$33 \pm 5$	2
KLS1L	2	46-60	
KLS1R	2	38-51	
KLS2L	2	50-55	
KLS2R	2	46-51	
KLS1L	44	176-198	
KLS1R	44	156-185	
KLS2L	44	182-203	
KLS2R	44	187-215	
KLS1L	66	270-315	
KLS1R	66	233-258	
$T = 500 \text{ }^\circ\text{C}$ , $P_f = 200 \text{ MPa}$			
11385	12	$133 \pm 114$	11
11185	8	$79 \pm 52$	5
11285	2	$43 \pm 29$	4
11985	1	$42 \pm 8$	6
103185	0.25	$9 \pm 8$	2
$T = 500 \text{ }^\circ\text{C}$ , $P_f = 150 \text{ MPa}$			
10485	0.5	<5	
10585	0.25	<5	
$T = 400 \text{ }^\circ\text{C}$ , $P_f = 200 \text{ MPa}$			
71185	8.5	$25 \pm 18$	3
31085	8	$30 \pm 18$	6
31285	6	$26 \pm 14$	5
71285	6	$21 \pm 5$	3
3985	4	12	1
31185	0.5	$14 \pm 9$	4
7885-2	0.5	11	1
10385	0.25	<5	

\* Samples beginning with K are from K. Shelton. Stated error in these measurements represent the range in  $a - r$  for each crack.

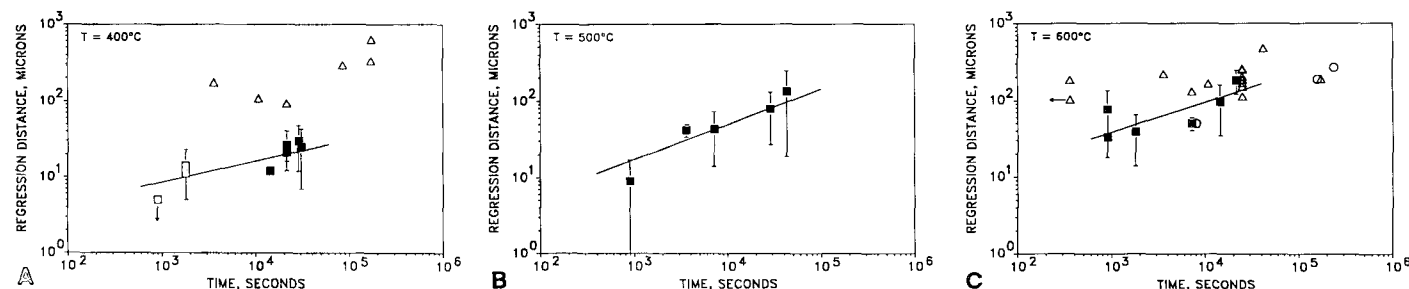
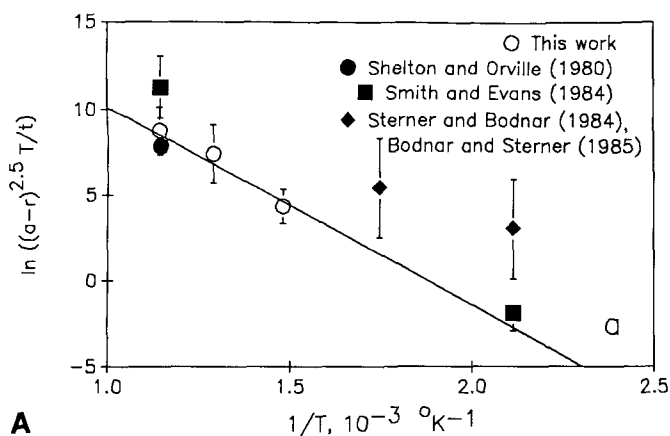
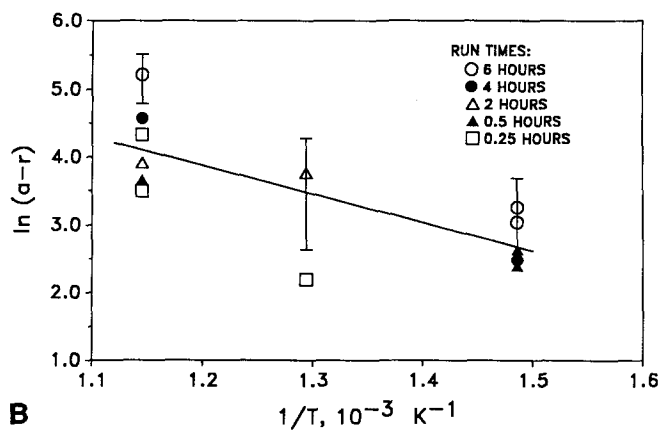


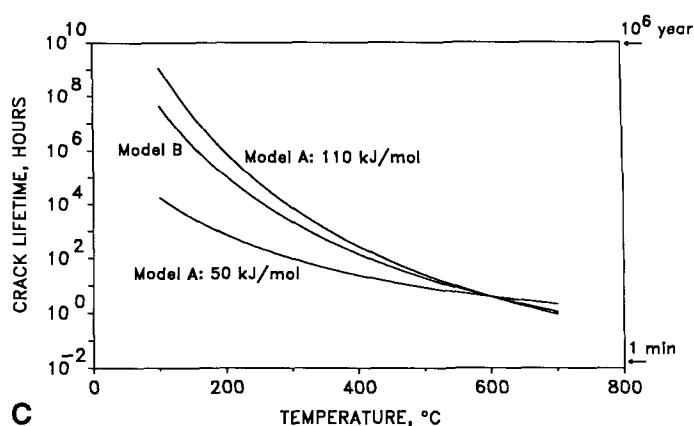
Figure 1. Measured crack-healing regression distances ( $a - r$ ) at water pressure ( $P_f$ ) = 200 MPa and (A) 400 °C, (B) 500 °C, and (C) 600 °C. Solid squares = this work; circles = Shelton and Orville (1980; also Shelton, 1985, personal commun.); triangles = Smith and Evans (1984). In C, data of Shelton and Orville at 2 h and those of Smith and Evans at 6 h have been shifted right for improved visibility. Lines represent best fits to our data (see text).



A



B



C

**Figure 2.** A: Calculated values of function  $\ln \{(a-r)^{1/n} T t^{-1}\}$  vs.  $1/T$ . See text for discussion of data points. Line shown represents linear fit to our data and those of Shelton and Orville (1980) (Table 1), weighted by inverse variance of  $a-r$  for each sample, and represents activation energy of  $80 \pm 26$  kJ/mol. B:  $\ln(a-r)$  vs.  $1/T$  at constant run time, using our data only (Table 1). Line shown represents apparent activation energy of about 35 kJ/mol. C: Extrapolated healing times as function of temperature for crack observed to heal completely in 4 h at 600 °C. Model A: using equation 1 with activation energies of 110 and 50 kJ/mol. Model B: assuming power-law time dependence and simple Arrhenius expression (equation 3) with apparent activation energy of 35 kJ/mol (see text).

and  $a-r$  in the range of 50 to 500  $\mu\text{m}$ , their data are higher than our predictions, although within error limits.

In Figure 2C, we have used equations 2 and 3 and our estimates of  $Q$  and  $Q^*$  to extrapolate to lower temperatures the lifetime of a microcrack observed to heal completely in 4 h at 600 °C. Both estimates assume that  $(a-r)$  is proportional to  $t^{0.4}$  (e.g., equation 1). At 200 °C, for example, the predicted healing times range from 30 days to 90 yr. Although the range of estimates is wide, both lifetimes are geologically short.

### Fluid Pressure and Chemistry Effects

The estimated lifetimes shown in Figure 2C are based on measured healing rates at  $P_f = P_c = 200$  MPa, and thus are valid only for pore fluids of similar chemistry at the same pressure. We observed that higher fluid pressure under hydrostatic conditions increases the healing rate at 500 °C. However, all our experiments were completed at  $P_f = P_c$ ; in regimes where quartz is subjected to nonhydrostatic stress, crack length will be a function of the competing rates of crack propagation and crack healing. Healing rates might also be seriously perturbed in two-phase regions of  $P$ - $T$  space.

Crack healing may also be affected by solution chemistry (Brantley and Voight, 1989). On the basis of precipitation rate, solubility, and surface-energy data (e.g., Iler, 1979; Parks, 1984; Dove and Crerar, unpub.), moderate increases in NaCl content and increases or decreases in pH could increase the healing rate, whereas dissolution-precipitation inhibitors (e.g., Fe, Al, Zn) and high mole fractions of nonaqueous phases could decrease the healing rate.

## CONCLUSIONS

### Healing Rates and Permeability

To illustrate the effect of crack healing on permeability, we calculated permeabilities for three hypothetical microcrack populations undergoing

healing (Fig. 3). We assumed an impermeable rock matrix and that all cracks are identical, elliptical in cross section, and extend to infinity in the direction parallel to the fluid-pressure gradient,  $\nabla P$ . We further assumed that we can use equation 1 with  $n = 0.4$ , even for slowly flowing fluids. The bulk (Darcian) permeability,  $k$ , is given by

$$|k| = \frac{\nu q}{\nabla P}, \quad (4)$$

where  $\nu$  is pore-fluid viscosity and  $q$  is the volume flow rate per unit area of rock. The flow rate through a single elliptical tube,  $q'$ , is

$$q' = \frac{\nabla P \pi a^3 b_r^3}{4\nu(a^2 + b_r^2)}, \quad (5)$$

where  $a$  and  $b_r$  are the semi-major and semi-minor axes (Lamb, 1932, p. 587). Permeabilities were calculated by combining equations 4 and 5 and assigning the same initial crack length,  $2a$ , and the same initial porosity to each population, and varying the maximum initial aperture,  $2b_r$ . When crack apertures are small, i.e., many thin microcracks, healing is rapid and the permeability decreases rapidly (Fig. 3). When the crack apertures are large, i.e., fewer but fatter cracks, the permeability is affected slowly. This simple model intentionally neglects several important factors in order to isolate and emphasize the importance of crack size and shape on the expected crack lifetime and their effect on permeability.

Because of the strong dependence of flow rate on fracture aperture, fluid flow is dominated by the transmissivity of large-scale fractures and joints. These features are connected to a network of finer interconnected pores and microcracks through which comparatively little fluid flows (Norton and Knapp, 1977). The two scales of porosity have vastly different lifetimes; larger fractures transport most of the fluid volume and seal slowly, whereas microcracks allow penetration of fluid into the rock mass but remain open only intermittently. The finer network provides the connections for the chemical and isotopic equilibration of the bulk of the rock.

In metamorphic regimes, fluid may flow through "metamorphic aquifers" where devolatilization reactions have caused hydrofractur-

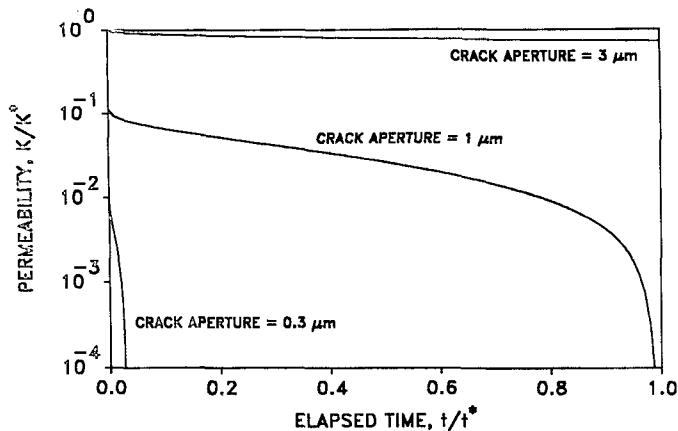


Figure 3. Calculated effect of crack healing on bulk permeability using equation 1, assuming monosized population of through-going elliptical cracks with maximum apertures ( $2b_1$ ) ranging from 3 to  $0.3 \mu\text{m}$  (see text);  $K^0$  is initial permeability of sample containing  $3 \mu\text{m}$  cracks, and  $t^*$  is lifetime of  $1\text{-}\mu\text{m}$ -aperture crack.

ing and enhancement of permeability beyond the normally low porosity (Rumble et al., 1982; Nabelek et al., 1984). One model for fluid flow in dehydrating regimes requires periods of hydrofracturing ( $P_f >$  least principal stress  $[\sigma_3] +$  rock tensile strength) in which fluid flows along fractures and microcracks, followed by rapid healing of cracks in moderately soluble minerals ( $P_f < \sigma_3$ ) (Vrolijk, 1987). As the microcracks are eliminated from the plumbing system, the surface area/water mass ( $A/M$ ) ratio for the system will become smaller and the equilibration times necessary for achievement of chemical, isotopic, and thermal equilibrium will lengthen (e.g., Rimstidt and Barnes, 1980).

#### Textural Equilibrium and Pore Shape

In the absence of other chemical and mechanical forces, e.g., in a given rock with stable, nonreacting phases where  $P_f = P_c$ , rock-pore structure can be determined by interfacial tension, which is a function of solution chemistry. For polycrystalline quartz with brine as a pore fluid at  $950\text{--}1150^\circ\text{C}$  and  $1 \text{ GPa}$ , the most stable pore structure is a completely connected network of tubes of triangular cross section that lies along grain corners. However, for mixed  $\text{H}_2\text{O-CO}_2$  fluids, unconnected pores are the stable morphology (Watson and Brenan, 1987). Equilibrium contact-angle geometries are established by solution-precipitation reactions similar to those controlling the crack-healing process; these processes allow fluid infiltration into a low-porosity rock. The fast rates of crack healing indicate that the curvature-driven processes responsible for infiltration should also be fast for quartz under crustal conditions. Preliminary work investigating contact-angle geometry in novaculite at  $600^\circ\text{C}$  and  $200 \text{ MPa}$  has revealed fast infiltration rates for brines (Lee et al., 1989).

The effects we have observed in our healing experiments and the predictions we can make from the model suggest that rates of solution-transfer reactions might be very important in determining both physical and chemical properties of rock-water systems. We conclude that more data concerning wetting, cracking, and healing of minerals in a variety of chemical solutions under crustal conditions will allow more accurate prediction of the weakening behavior and the nature of porosity and permeability of rocks.

#### REFERENCES CITED

- Bodnar, R.J., and Sterner, S.M., 1985, Synthetic fluid inclusions in natural quartz. II. Application to  $PVT$  studies: *Geochimica et Cosmochimica Acta*, v. 49, p. 1855-1859.  
 — 1987, Synthetic fluid inclusions, in Ulmer, G.C., and Barnes, H.L., eds., *Hydrothermal experimental techniques*: New York, John Wiley, p. 423-457.

- Brantley, S.L., and Voigt, D., 1989, Fluid chemistry and microcrack healing in quartz [abs.]: *Eos (Transactions, American Geophysical Union)*, v. 70, p. 502.  
 Evans, A.G., and Charles, E.A., 1977, Strength recovery by diffusive crack healing: *Acta Metallurgica*, v. 25, p. 919-927.  
 Ferry, J.M., 1986, Reaction progress: A monitor of fluid-rock interaction during metamorphic and hydrothermal events, in Walther, J.V., and Wood, B.J., eds., *Fluid-rock interactions during metamorphism*: New York, Springer-Verlag, p. 60-88.  
 Heard, H.C., and Page, L., 1982, Elastic moduli, thermal expansion and inferred permeability of two granites to  $350^\circ\text{C}$  and  $55 \text{ MPa}$ : *Journal of Geophysical Research*, v. 87, p. 9340-9348.  
 Hickman, S.H., and Evans, B., 1987, Diffusional crack healing in calcite: The influence of crack geometry upon healing rate: *Physics and Chemistry of Minerals*, v. 15, p. 91-102.  
 Iler, R.K., 1979, *The chemistry of silica: Solubility, polymerization, colloid and surface properties and biochemistry*: New York, Wiley-Interscience, 866 p.  
 Lamb, H., 1932, *Hydrodynamics*: Cambridge, Cambridge University Press, 738 p.  
 Lasaga, A.C., 1984, Chemical kinetics of water-rock interactions: *Journal of Geophysical Research*, v. 89, p. 4009-4025.  
 Lee, V., Mackwell, S.J., and Brantley, S.L., 1989, Effect of fluid chemistry on the wetting of quartzite [abs.]: *Eos (Transactions, American Geophysical Union)*, v. 70, p. 502.  
 Martin, R.J., 1972, Time-dependent crack growth in quartz and its application to creep of rocks: *Journal of Geophysical Research*, v. 77, p. 1406-1419.  
 Nabelek, P.I., Labotka, T.C., O'Neil, J.R., and Papike, J.V., 1984, Contrasting fluid/rock interaction between the Notch Peak granitic intrusion and argillites and limestones in western Utah: Evidence from stable isotopes and phase assemblages: *Contributions to Mineralogy and Petrology*, v. 86, p. 25-34.  
 Norton, D., and Knapp, R., 1977, Transport phenomena in hydrothermal systems: The nature of porosity: *American Journal of Science*, v. 277, p. 913-936.  
 Parks, G., 1984, Surface and interfacial free energies of quartz: *Journal of Geophysical Research*, v. 89, p. 3997-4008.  
 Rimstidt, J.D., and Barnes, H.L., 1980, The kinetics of silica-water reactions: *Geochimica et Cosmochimica Acta*, v. 44, p. 1683-1699.  
 Roedder, E., 1981, Origin of fluid inclusions and changes that occur after trapping, in Hollister, L.S., and Crawford, M.L., eds., *Fluid inclusions: Applications to petrology*: Mineralogical Association of Canada Short Course Handbook, v. 6, p. 101-337.  
 — 1984, *Fluid inclusions: Mineralogical Society of America Reviews in Mineralogy*, v. 12, p. 70-77.  
 Rumble, D., Ferry, J.M., Hoering, T.C., and Boucot, A.J., 1982, Fluid flow during metamorphism at the Beaver Brook fossil locality, N.H.: *American Journal of Science*, v. 282, p. 886-919.  
 Shelton, K.L., and Orville, P.M., 1980, Formation of synthetic fluid inclusions in natural quartz: *American Mineralogist*, v. 65, p. 1233-1236.  
 Simmons, G., and Richter, D., 1976, Microcracks in rocks, in Strens, R.G.J., ed., *The physics and chemistry of minerals and rocks*: New York, Wiley-Interscience, p. 105-137.  
 Smith, D.L., and Evans, B., 1984, Diffusional crack healing in quartz: *Journal of Geophysical Research*, v. 89, p. 4125-4135.  
 Sterner, S.M., and Bodnar, R.J., 1984, Synthetic fluid inclusions in natural quartz I. Compositional types synthesized and applications to experimental geochemistry: *Geochimica et Cosmochimica Acta*, v. 48, p. 2659-2668.  
 Vrolijk, P., 1987, Tectonically driven fluid flow in the Kodiak accretionary complex, Alaska: *Geology*, v. 15, p. 466-469.  
 Walder, J., and Nur, A., 1984, Porosity reduction and crustal pore pressure development: *Journal of Geophysical Research*, v. 89, p. 11,539-11,548.  
 Walther, J.V., and Orville, P.M., 1982, Volatile production and transport in regional metamorphism: *Contributions to Mineralogy and Petrology*, v. 79, p. 252-257.  
 Walther, J.V., and Wood, B.J., 1984, Rate and mechanism in prograde metamorphism: *Contributions to Mineralogy and Petrology*, v. 81, p. 246-259.  
 Watson, E.B., and Brenan, J.M., 1987, Fluids in the lithosphere. I: Experimentally determined wetting characteristics of  $\text{CO}_2\text{-H}_2\text{O}$  fluids and their implications for fluid transport, host-rock physical properties, and fluid-inclusion formation: *Earth and Planetary Science Letters*, v. 85, p. 497-515.

#### ACKNOWLEDGMENTS

Funded by National Science Foundation Grant EAR-84-19421 to Evans and Crerar and Grant EAR-86-57868 to Brantley. We thank K. Shelton for access to unpublished healing data, L. S. Hollister for helpful discussion, and J. V. Walther for a useful review.

Manuscript received March 10, 1989

Revised manuscript received August 30, 1989

Manuscript accepted September 8, 1989